PHASE TRANSITIONS IN INSERTION ELECTRODES FOR LITHIUM BATTERIES

by

Michael M. Thackeray
Electrochemical Technology Program, Chemical Technology Division,
Argonne National Laboratory, Argonne, Illinois 60439, USA

September 1999

To be published in the Proceedings Volume of the American Ceramics Society:

DISCLAIMER

DISCLAIMER

Portions of this document may be illegible in electronic image products. Images are produced from the best available original document.

Phase Transitions in Insertion Electrodes for Lithium Batteries

by

Michael M. Thackeray
Electrochemical Technology Program, Chemical Technology Division,
Argonne National Laboratory, Argonne, Illinois 60439, USA

Abstract

Phase transitions that occur during lithium insertion into layered and framework structures are discussed in the context of their application as positive and negative electrodes in lithium-ion batteries. The discussion is focused on the two-dimensional structures of graphite, $LiNi_{1-x}M_xO_2$ (M=Co, Ti and Mg), and $Li_{1.2}V_3O_8$; examples of framework structures with a three-dimensional interstitial space for Li^+-ion transport include the spinel oxides and intermetallic compounds with zinc-blende-type structures. The phase transitions are discussed in terms of their tolerance to lithium insertion and extraction and to the chemical stability of the electrodes in the cell environment.

Keywords: insertion electrode, lithium battery, structure, phase transition

Introduction

Lithium-ion batteries operate by an electrochemical process by which lithium ions are shuttled between two host electrodes during charge and discharge [1]. During charge, the host structures of the negative (anode) and positive (cathode) electrodes are reduced and oxidized, respectively; these processes are reversed during discharge. The repeated insertion and extraction of lithium with these host structures often subject them to structural damage and to the decay of their surfaces by chemical reaction with the electrolyte. Moreover, the change in composition of the electrodes, Li_xH (where H represents the host structure), necessitates electron transfer and a change in the formal oxidation state of the host. Lithium insertion or extraction from these compounds produces metastable structures over a wide compositional range, thereby affecting the

chemical stability of the electrode in the cell environment. For example, metal oxide positive electrodes such as Li_xCoO_2 and $Li_xMn_2O_4$ become highly oxidizing materials at low lithium levels and provide a high potential (~4 V) vs. metallic lithium. In contrast, lithium insertion into carbon, such as graphite, occurs at a potential close to that of metallic lithium, resulting in a highly reducing electrode, LiC_6, when fully charged. Selection of insertion electrodes for lithium batteries thus requires structures that are as tolerant to lithium insertion over as wide a compositional range as possible without compromising their chemical stability and the cycle life of the lithium cell.

Many compounds that are of interest as insertion electrodes for lithium batteries have close-packed structures with a two-dimensional or three-dimensional interstitial space for lithium transport [2]. Tunnel structures have not received much prominence because their one-dimensional channels tend to restrict the rate of lithium diffusion and the amount of lithium that can be accommodated within their structures. A good example of such a tunnel structure is β-MnO_2 with a rutile-type structure; the rutile host can accommodate only 0.2 Li^+ ions within its interstitial space before it transforms irreversibly to the $[Mn_2]O_4$ spinel framework [2, 3]. This paper therefore focuses on various layered and structure types to emphasize those features that account for the structural and chemical stability (or instability) of lithium insertion electrodes under the operating conditions of a lithium cell. The materials with a two-dimensional space for lithium diffusion include graphite, $LiNi_{1-x}M_xO_2$ (M=Co, Ti and Mg), and $Li_{1.2}V_3O_8$. Examples of structures with three-dimensional pathways for lithium include the spinel oxides $Li_4Ti_5O_{12}$ and $LiMn_2O_4$, and intermetallic compounds with zinc-blende-type structures such as InSb.

Negative Electrodes (Anodes)

1. Graphite

Graphite is the negative electrode material of choice for lithium-ion batteries. The reasons for this are two-fold: 1) a lithiated graphite electrode, Li_xC_6 ($x \leq 1$), provides most of its capacity close to that of metallic lithium, yielding high cell voltage and energy, and 2) the graphite structure can accommodate one lithium per C_6 unit reversibly over many cycles without a significant capacity loss.

A schematic illustration of the layered graphite structure is shown in Fig. 1a. Lithium is inserted in between the carbon sheets in a staged process, during which the close-packed carbon atoms shear from their hexagonal-close-packed stacking ABABAB (occasionally cubic-close packed stacking ABCABC) to AAAAAA stacking, as illustrated in Fig. 1b [4]. Steric constraints in the ideal graphite structure limit the amount of inserted lithium to one per six carbons, i.e., LiC_6, in which every third C_6 hexagon has one lithium atom above the center of the hexagon (Fig. 1b).

The hexagonal unit cell of graphite expands anisotropically on lithiation, as reflected predominantly by the spacing between the carbon sheets that increases by 10.4% from 3.36 Å in graphite to 3.71 Å in LiC_6. Because the anisotropic breathing of the crystal lattice is not severe enough to damage the structural integrity of the electrode during electrochemical cycling, graphite is an attractive negative insertion electrode for lithium-ion batteries.

Because lithiated graphite, Li_xC_6, operates close to the potential of metallic lithium, it is a highly reactive (reducing) material, particularly toward the organic electrolyte solvents of lithium-ion cells. Fortunately, a passive, protective film consisting of numerous species, such as oxides, hydroxides, carbonates, and fluorides, is formed by reaction of Li_xC_6 with the electrolyte, and protects the negative electrode from further reaction. Nevertheless, there is a concern about the inherent safety of Li-ion cells because of the possibility of thermal runaway if they are abused or not protected from overcharge. A significant research effort is, therefore, being made to find alternative host structures for lithium that operate a few hundred millivolts above that of metallic lithium to reduce the safety risk.

2. *Zinc-blende-type intermetallic compounds*

Much effort has been spent to develop metal alloy systems, such as Li_xAl, Li_xSi, and Li_xSn, to reduce the activity of the lithium electrode [5-8]. A major problem of these binary alloy systems is that their structures expand severely on lithiation, thus placing a major limitation on their cycling efficiency. This problem can be partially overcome by using composite electrodes in which the alloy system is embedded in an inactive phase. Examples of such composite electrodes include those derived from amorphous tin oxide

in which Li_xSn grains are embedded in a Li_2O matrix [9, 10], or from electrochemically co-deposited intermetallic systems such as Sn_xAg_y [11].

It was recently announced that certain ternary intermetallic compounds Li_xMM' in which a MM′ zinc-blende framework structure containing two types of metal atoms, M and M′, can accommodate a significant quantity of lithium without undergoing a damaging volumetric change [12]. A good example is face-centered-cubic InSb (space group F-43m) shown in Fig. 2a. The InSb zinc-blende-type structure has a diamond network in which each In atom is surrounded by four Sb atoms in tetrahedral coordination, and vice versa. The interstitial space of InSb consists of a network of interconnected, hexagonally shaped tunnels; the tunnels in the [110] crystallographic direction are shown in Fig. 2b. The interstitial space of InSb contains two crystallographically independent sites for lithium at the (½, ½, ½) and (□,□,□) positions of the unit cell (Fig. 2c). Lithium is inserted electrochemically into InSb in a two-stage process; it has been proposed that the lithium fills the two independent sites to yield LiInSb and Li_2InSb, the latter product having a structure related to Heusler-type phases [13]. There is very little volume change associated with these phase transformations; moreover, the reactions are reversible. Further reaction of lithium with Li_2InSb displaces In from the structure according to the reaction:

$$x\,Li + Li_2InSb \leftrightarrow Li_{2+x}In_{1-x}Sb + x\,In \qquad (1)$$

This displacement reaction is also readily reversible at room temperature [12].

The compound Li_2CuSn is isostructural with Li_2InSb. However, in this case, the CuSn zinc-blende framework is unstable to lithium extraction; the removal of lithium is accompanied by an internal displacement of one-half of the Sn atoms to yield a "CuSn" product with a NiAs-type structure [14, 15]. Although this reaction is reversible, the diffusion of the tin atoms and the less favorable interstitial space for Li diffusion in NiAs-type structures limit the performance of Li_2CuSn electrodes.

3. *$Li_4Ti_5O_{12}$*

This compound has a spinel-type structure (Fig. 3a) that can be represented in spinel notation as $Li[Li_{0.33}Ti_{1.67}]O_4$. It has cubic symmetry Fd3m. The lithium ions outside the square brackets refer to the tetrahedral A-site cations of an $A[B_2]O_4$ spinel, whereas the

lithium and titanium ions within the brackets refer to octahedral B-site cations. Lithium insertion into $Li[Li_{0.33}Ti_{1.67}]O_4$ is accompanied by a first-order phase transition to the rock salt phase $Li_2[Li_{0.33}Ti_{1.67}]O_4$ (Fig. 3b), during which the tetrahedral-site lithium ions are cooperatively displaced into neighboring octahedral sites [16, 17]. The two-phase reaction provides a constant voltage response at approximately 1.5 V vs. lithium. The cubic symmetry is unaffected by the phase transition; moreover, the lattice parameter (8.36 Å in $Li_4Ti_5O_{12}$) is essentially unaffected by lithiation, expanding by only 0.1% (to 8.37 Å). As a result, the $Li_4Ti_5O_{12}$ electrode provides outstanding structural stability for many hundreds of cycles. The excellent structural and chemical stability of $Li_{4+x}Ti_5O_{12}$ under the working conditions of the cell represent characteristics of an ideal insertion electrode. Because of its relatively low voltage vs. lithium, $Li_4Ti_5O_{12}$ is not used as a positive electrode in practical lithium cells; this compound is of greater interest as a negative electrode because it is safe compared to metallic lithium and LiC_6 electrodes, and because it can be coupled with "4 V" positive electrodes such as $LiCoO_2$ and $LiMn_2O_4$ or "3 V" Li_xMnO_2 electrodes to provide 2.5 V and 1.5 V cells, respectively [18].

Positive Electrodes (Cathodes)

1. Layered Oxides: $LiNi_{1-x}M_xO_2$

State-of-the-art Li-ion cells use $LiCoO_2$ as the positive electrode because of the relative ease of preparing a high-quality layered structure (space group symmetry R-3m) and because $LiCoO_2$ is stable to lithium extraction over a wide compositional range ($0.5 \leq x < 1.0$) in $Li_{1-x}CoO_2$ [19, 20]. The high cost of cobalt has encouraged the lithium battery industry to develop an isostructural $LiNiO_2$ electrode. Lithium extraction from $LiNiO_2$ is accompanied by a series of phase transitions. Three hexagonal phases, labeled H(1), H(2), and H(3), exist over the range $0 \leq x \leq 1$ in $Li_{1-x}NiO_2$ [21, 22]. A distorted monoclinic phase that has been attributed to ordering of the Li ions has been reported to occur between H(1) and H(2) for $0.2 < x < 0.55$ [22], although evidence of this phase is not always observed [23]. The H(1)-to-H(2), and H(2)-to-H(3) transitions are manifest by changes in the crystallographic *c/a* ratios of the lattice parameters. The H(1)-to-H(2) transition is small and subtle, and results in minor changes to the unit cell without

disturbing the Ni ions from their octahedral sites. By contrast, the H(2)-to-H(3) transition is accompanied by a major contraction of the *c* lattice parameter [23]. This transition takes place at x≈0.75 when the lithium content is relatively low and the Ni^{4+} content is relatively high, and is believed to account for much of the structural damage to the electrode and consequent loss in capacity on cycling $Li_xC_6/Li_{1-x}NiO_2$ cells.

Unfortunately, $LiNiO_2$ with the ideal layered configuration (Fig. 4) is more difficult to prepare than $LiCoO_2$; $LiNiO_2$ products often contain some Ni within the Li layers that tends to reduce its quality as an insertion electrode, both in terms of delivered capacity and cyclability. Moreover, Ni^{4+} is more highly oxidizing than Co^{4+}, leading to higher reactivities with the organic electrolytes at the top of charge. Much effort has thus been made to stabilize the $LiNiO_2$ structure by cation substitution. One such example is $LiNi_{0.65}Co_{0.25}Ti_{0.05}Mg_{0.05}O_2$ which has improved the electrochemical performance and cycling stability of the lithium-ion cells [24]. In this compound, (1) the Co ions (25%) stabilize the layered configuration; (2) the Ti^{4+} ions (5%) provide strong Ti-O bonds that strengthen the oxygen array and thereby reduce oxygen loss at the top of charge; and (3) the Mg^{2+} ions (5%) compensate for the charge imbalance introduced by the Ti^{4+} ions and enhance the electrical properties of the electrode, as they do in substituted $LiCo_{1-x}Mg_xO_2$ compounds [25]. All the lithium cannot be extracted electrochemically from $Li_{1-x}Ni_{0.65}Co_{0.25}Ti_{0.05}Mg_{0.05}O_2$ electrodes because the transition metal ions become fully oxidized at the composition $Li_{0.1}Ni_{0.65}Co_{0.25}Ti_{0.05}Mg_{0.05}O_2$. The H(2)-to-H(3) phase transition in such substituted electrodes is, therefore, suppressed. Consequently, the H(2)-to-H(3) phase transition is accompanied by relatively minor changes to both the *a* and *c* lattice parameters; the resulting electrode has significantly enhanced structural stability over a wide compositional range.

2. *$Li_{1.2}V_3O_8$*

The lithium vanadium oxide, $Li_{1.2}V_3O_8$, is of interest as a positive electrode for 2.5 V lithium cells with metallic lithium anodes [26, 27]. The structural and electrochemical properties of the $Li_{1.2}V_3O_8$ electrode have been investigated in detail [26-30]. Figure 5a shows the layered structure of $Li_{1.2}V_3O_8$. The structure has monoclinic symmetry ($P2_1/m$). There are three crystallographically independent V atoms

in the unit cell, two of which reside in distorted octahedra; the third V atom has square pyramidal coordination [29, 30]. The V polyhedra are connected to one another in sheets. The 1.2 Li^+ ions reside between the sheets, one Li^+ ion fully occupying an octahedral site, and the remaining 0.2 Li^+ ions partially occupying one crystallographically independent tetrahedral site in the unit cell. The lithium layers also contain several empty distorted tetrahedra that constitute the interstitial space of the $Li_{1.2}V_3O_8$ structure.

The mechanisms whereby lithium is inserted into $Li_{1.2}V_3O_8$ have been studied by electrochemical techniques [28], single-crystal structure analysis [30], and theoretical *ab initio* structure calculations [31, 32]. These studies have shown that lithium can be inserted readily to a composition $Li_4V_3O_8$, the structure of which is shown in Fig. 5b, and to the stoichiometric rock salt composition $Li_5V_3O_8$ under slow electrochemical titration [28]. These studies have shown that the lithium insertion follows a reaction sequence similar to that observed in the lithium spinels. Lithium is first inserted in a series of single-phase processes (i.e., with a sloping voltage profile) into the tetrahedral sites of $Li_{1.2}V_3O_8$, the sequence of which has been predicted by theoretical calculations of site energies in $Li_{1+x}V_3O_8$ to a composition $Li_3V_3O_8$ [32]. When additional lithium is introduced, the lithium ions in both the tetrahedral and octahedral sites are cooperatively displaced into neighboring octahedral sites in a two-phase reaction (constant voltage) to provide a defect rock salt phase of composition $Li_4V_3O_8$, in which all the vanadium ions are tetravalent; thereafter, the remaining octahedral sites are occupied in another two-phase reaction to yield the stoichiometric rock-salt composition $Li_5V_3O_8$. Small adjustments to the oxygen array are made during the transitions from $Li_{2.5}V_3O_8$ to $Li_4V_3O_8$ and to $Li_5V_3O_8$ which place all the V ions in octahedral coordination without any significant disturbance to the V_3O_8 sublattice or change to the monoclinic crystal symmetry. In the transitions from $Li_{1.2}V_3O_8$ to $Li_4V_3O_8$, the *b* and *c* lattice parameters expand by 9.9% and 0.4%, respectively, whereas the *a* lattice parameter contracts by 9.7% [30]. Although the unit cell volume is unaffected by lithium insertion (it changes from 265.36 to 265.33 $Å^3$), the anisotropic change in lattice parameters is sufficient to cause cracking of the particles, particularly if lithiation is carried out chemically with a strong lithiating agent such as n-butyl lithium [33]. Nevertheless, because of the

excellent stability of the V_3O_8 sublattice to "soft" electrochemical lithiation, $Li_{1.2}V_3O_8$ remains an excellent candidate for rechargeable 2.5 V lithium cells.

3. $LiMn_2O_4$

The spinel system $Li_x[Mn_2]O_4$ is attractive as an insertion electrode because the $[Mn_2]O_4$ spinel framework, which provides a three-dimensional space for Li^+-ion diffusion, is stable over a wide compositional range ($0 \leq x \leq 2$) [34-38]. The range $0 \leq x < 1$ is particularly attractive for two reasons. First, the symmetry of $Li_x[Mn_2]O_4$ remains cubic (Fd3m), allowing the unit cell to breathe isotropically and to maintain structural stability, despite an order-disorder transition of the lithium ions on the tetrahedral sites at $Li_{0.5}[Mn_2]O_4$ [39]. Second, the electrode provides a high voltage (4 V) vs. lithium over this range, thereby yielding cells with high specific energy and a high power capability. Over the range $1 < x \leq 2$, a first-order phase transition occurs during which the lithium ions on tetrahedral sites in $Li[Mn_2]O_4$ (Fig. 3a) are cooperatively displaced into neighboring octahedral sites to generate the rock salt phase $Li_2[Mn_2]O_4$ (Fig. 3b) [34]; this reaction occurs at a constant 3 V. The phase transition induces a Jahn-Teller distortion in the MnO_6 octahedra that reduces the crystal symmetry from cubic in $Li[Mn_2]O_4$ to tetragonal ($F4_1/ddm$) in $Li_2[Mn_2]O_4$. The *c/a* ratio changes by 16%, which, crystallographically, is far too severe for the $Li_x[Mn_2]O_4$ electrode to maintain its structural integrity on cycling at 3 V [38]. The stability of the spinel electrode at 3 V can be significantly improved by changing the composition of the electrode; for example, some of the manganese in the spinel framework can be replaced by a monovalent, divalent, or trivalent cation such as Li^+, Mg^{2+}, and Al^{3+} [40]. This change in composition increases the Mn^{4+} content in the spinel electrode, which eliminates the Jahn-Teller effect at the beginning of discharge at 3 V, and reduces the magnitude of the effect in its fully discharged state [41]. However, stability of the electrode at 3 V is gained at the expense of capacity at 4 V.

Phase changes in lithium-metal-oxide insertion electrodes, in which the composition of the electrode and oxidation state of the metal ions are both being continuously varied, can be also induced by chemical decomposition or reaction with the cell electrolyte. These phase transitions can be particularly evident at the top of charge or at the end of discharge when the metal oxide is in a highly oxidized or reduced state. A good example

of a chemically induced phase transition is provided by the $Li_x[Mn_2]O_4$ spinel electrode when cycled over the high voltage regions (above 3 V). Even though the cubic $[Mn_2]O_4$ spinel framework provides a structurally robust framework for lithium insertion and extraction, $Li/Li_x[Mn_2]O_4$ cells still lose capacity slowly when cycled over this voltage regime [40, 42]. The primary reason for this capacity fade has been attributed to solubility of the electrode in common electrolytes, such as 1M $LiPF_6$ in ethylene carbonate, dimethyl carbonate; these electrolytes contain acidic species such as HF, formed by hydrolysis of the lithium salt with residual water in the electrolyte [43, 44]. Following the early work of Hunter [45], it is generally acknowledged that the solubility of $Li_x[Mn_2]O_4$ electrodes in acid medium occurs by the disproportionation reaction

$$Mn^{3+}_{(solid)} \rightarrow Mn^{4+}_{(solid)} + Mn^{2+}_{(solution)} \qquad (2)$$

during which the Mn^{2+} ions go into solution, and the Mn^{4+} ions remain in the solid spinel phase.

Full electrochemical delithiation of $Li[Mn_2]O_4$ leaves λ-MnO_2 with the $[Mn_2]O_4$ spinel framework. Like many manganese dioxides, λ-MnO_2 is a powerful oxidizing agent and can be readily reduced. Therefore, any oxygen that may be evolved at the particle surface of the spinel electrode at the top of charge will result in Mn^{3+} ions at the electrode surface; the instability of Mn^{3+} ions at the high potential of the charged cell will also drive the solubility reaction (2) shown above, thus damaging the spinel surface and resulting in some irreversible capacity loss to the cell.

The presence of tetragonal $Li_2[Mn_2]O_4$ has been observed in very small amounts at the surface of $Li[Mn_2]O_4$ spinel electrodes at the end of discharge after high rate cycling (C/3 rate) between 4.2 and 3.3 V vs. Li [46]. The presence of $Li_2[Mn_2]O_4$ on the electrode surface 300 mV above the thermodynamically expected voltage for this phase has been attributed to a localized overpotential at the electrode surface during high-rate discharge and to an inhomogeneous lithiation of the spinel surface. The compound $Li_2[Mn_2]O_4$, in which all the manganese ions are trivalent, will be unstable, like $Li[Mn_2]O_4$, in a 1M $LiPF_6$/EC/DMC electrolyte. In this case, a disproportionation reaction occurs in which MnO dissolves from the particle surface to leave an insoluble and stable Li_2MnO_3 rock-salt phase. This reaction accounts for some of the capacity loss of 4-V $Li/Li_x[Mn_2]O_4$ cells on long-term cycling [47].

Concluding Remarks

Phase transitions that occur in lithium insertion electrodes during the cycling of lithium cells tend to be damaging phenomena. Optimum stability to lithium insertion and cycle life are generally obtained from those systems that undergo minimum crystallographic changes, such as to crystal symmetry, lattice parameters, and unit cell volume, and from those systems where there is no diffusion of the atoms of the host framework structure. Moreover, the host structures must be chemically stable to the cell electrolyte at all states of charge and discharge, when the composition and oxidation state of the electrode are continuously changing. From the viewpoint of structural and chemical stability with respect to lithium battery electrolytes, the cubic spinel system $Li[Ti_{1.67}Li_{1.33}]O_4$ represents an ideal host electrode because 1) the $[Ti_{1.67}Li_{1.33}]O_4$ host framework remains intact during lithiation, 2) the host framework breathes isotropically during the cubic-$Li[Ti_{1.67}Li_{1.33}]O_4$ to cubic-$Li_2[Ti_{1.67}Li_{1.33}]O_4$ transition with virtually no change to the lattice parameter, and hence volume, and 3) the $Li_{1+x}[Ti_{1.67}Li_{1.33}]O_4$ electrode (x=0 and x=1) is chemically stable and can tolerate hundreds of deep discharge cycles with little capacity fade.

Acknowledgments

J. T. Vaughey is thanked for providing the illustrations of the various structures. Support for writing this article from the Chemical Sciences Division, Office of Basic Energy Sciences of the United States Department of Energy under Contract No. W31-109-Eng-38 is gratefully acknowledged.

References

1. M. Winter, J. O. Besenhard, M. E. Spahr and P. Novak, *Insertion Electrode Materials for Rechargeable Lithium Batteries*, Adv. Mater., **10**, 725-763 (1998).
2. M. M. Thackeray, *The Structural Stability of Transition Metal Oxide Electrodes for Lithium Batteries*, in Handbook of Battery Materials (Ed. J. O. Besenhard), Wiley-VCH, pp. 293-317 (1999).
3. D. W. Murphy, F. J. Di Salvo, J. N. Carides and J. V. Waszczak, *Topochemical Reactions of Rutile Related Structures with Lithium*, Mat. Res. Bull., **13**, 1395-1402 (1978).
4. J. R. Dahn, A. K. Sleigh, Hang Shi, B. M. Way, W. J. Weydanz, J. N. Reimers, Q. Zhong and U. von Sacken, *Carbons and Graphites as Substitutes for the Lithium Anode*, in Lithium Batteries (Ed. G. Pistoia), Elsevier, Amsterdam, 1-47 (1994).
5. D. Fauteux and R. Koksbang, *Rechargeable Lithium Battery Anodes: Alternatives to Metallic Lithium*, J. Appl. Electrochem., **23**, 1-10 (1993).
6. J. Wang, I. D. Raistrick and R. A. Huggins, *Behavior of Some Binary Alloys as Negative Electrodes in Organic Solvent-Based Electrolytes*, J. Electrochem. Soc., **133**, 457-460 (1986).
7. J. O. Besenhard, P. Komenda, A. Paxinos, E. Wudy and M. Josowicz, *Binary and Ternary Li-Alloys as Anode Materials in Rechargeable Li-Batteries*, Solid State Ionics, **18&19**, 823-827 (1986).
8. Y. Idota, T. Kubota, A. Matsufiji, Y. Maekawa and T. Miyasaka, *Tin-Based Amorphous Oxide: A High-Capacity Lithium-Ion-Storage Material*, Science, **276**, 1395-1397 (1997).
9. I. A. Courtney and J. R. Dahn, *Electrochemical and In Situ X-Ray Diffraction Studies of the Reaction of Lithium with Tin Oxide Composites*, J. Electrochem. Soc., **144**, 2045-2052 (1997).
10. J. Yang, M. Winter and J. O. Besenhard, *Small Particle Size Multiphase Li-Alloy Anodes for Lithium-Ion Batteries*, Solid State Ionics, **90**, 281-287 (1996).
11. J. O. Besenhard, J. Yang and M. Winter, *Will Advanced Lithium-Alloy Anodes Have a Chance in Lithium-Ion Batteries?* J. Power Sources, **68**, 87-90 (1997).
12. J. T. Vaughey, J. O'Hara and M. M. Thackeray, *Intermetallic Insertion Electrodes with a Zinc-Blende-Type Structure for Li Batteries: A Study of Li_xInSb ($0 \leq x < 3$)*, Electrochemical and Solid State Letters, (1999). Submitted.
13. P. J. Webster, K. R. A Ziebeck, S. L. Town and M. S. Peak, *Magnetic Order and Phase Transformation in Ni_2MnGa*, Phil. Mag. B, **49**, 295-310 (1984).
14. K. D. Kepler, J. T. Vaughey and M. M. Thackeray, *$Li_xCu_6Sn_5$ ($0 < x < 13$): An Intermetallic Insertion Electrode for Rechargeable Lithium Batteries*, Electrochemical and Solid State Letters, **2**, 307-309 (1999).
15. J. T. Vaughey, K. D. Kepler, R. Benedek and M. M. Thackeray, *NiAs- vs. Zinc-Blende-type Intermetallic Insertion Electrodes for Lithium Batteries; Lithium Extraction from Li_2CuSn*, Electrochem. Comm., (1999). Submitted.
16. K. M. Colbow, J. R. Dahn and R. R. Haering, *Structure and Electrochemistry of the Spinel Oxides $LiTi_2O_4$ and $Li_4Ti_5O_{12}$*, J. Power Sources, **26**, 397-402 (1989).

17. T. Ohzuku, A. Ueda and N. Yamamoto, *Zero-Strain Insertion Material of $Li[Li_{1/3}Ti_{5/3}]O_4$ for Rechargeable Lithium Cells*, J. Electrochem. Soc., **142**, 1431-1435 (1995).
18. E. Ferg, R. J. Gummow, A. de Kock and M. M. Thackeray, *Spinel Anodes for Lithium-Ion Batteries*. J. Electrochem. Soc., **141**, L147-L150 (1994).
19. K. Mizushima, P. C. Jones, P. J. Wiseman and J. B. Goodenough, *$LiCoO_2$ ($0<x\leq1$): A New Cathode Material for Batteries of High Energy Density*, Mat. Res. Bull., **15**, 783-789 (1980).
20. T. Ohzuku and A. Ueda, *Solid-State Redox Reactions of $LiCoO_2$ (R-3m) for 4 V Secondary Lithium Cells*, J. Electrochem. Soc., **141**, 2972-2977 (1994).
21. T. Ohzuku, A. Ueda and M. Nagayama, *Electrochemistry and Structural Chemistry of $LiNiO_2$ (R-3m) for 4 V Secondary Lithium Cells*, J. Electrochem. Soc., **140**, 1862-1870 (1993).
22. W. Li, J. N. Reimers and J. R. Dahn, *In Situ X-ray Diffraction and Electrochemical Studies of $Li_{1-x}NiO_2$*, Solid State Ionics, **67**, 123-130 (1993).
23. X. Q. Yang, X. Sun and J. McBreen, *New Findings on the Phase Transitions in $Li_{1-x}NiO_2$: In-situ Synchrotron X-ray Diffraction Studies*, Electrochem. Comm., **1**, 227-232 (1999).
24. X. Sun, X. Q. Yang, J. McBreen, Y. Gao, M. V. Yakovleva, X. K. Xing and M. L. Daroux, *Studies on Relationship Between Structure of $LiNiO_2$ Based Cathode Materials and Thermal Stabilities at Over-Charged State*, Ext. Abstr., No. 389, 196th Electrochem. Soc. Meeting, Hawaii, Oct 17-22, 1999.
25. H. Tukamoto and A. R. West, *Electronic Conductivity of $LiCoO_2$ and Its Enhancement by Magnesium Doping*, J. Electrochem. Soc., **144**, 3164-3168 (1985).
26. G. Pistoia, M. Pasquali, M. Tocci, R. V. Moshtev and V. Manev, *$Li/Li_{1+x}V_3O_8$ Secondary Batteries: Further Characterization of the Mechanism of Li^+ Insertion and of the Cycling Behavior*, J. Electrochem. Soc., **132**, 281-284 (1985).
27. G. Pistoia, M. Pasquali, G. Wang and L. Li, *$Li/Li_{1+x}V_3O_8$ Secondary Batteries: Synthesis and Characterization of an Amorphous Form of the Cathode*, J. Electrochem. Soc., **137**, 2365-2370 (1985).
28. K. West, B. Zachau-Christiansen, S. Skaarup, Y. Saidi, J. Barker, I. I. Olsen, R. Pynenburg and R. Koksbang, *Comparison of LiV_3O_8 Cathode Materials Prepared by Different Methods*, J. Electrochem. Soc., **143**, 820-825, (1996).
29. A. D. Wadsley, *Crystal Chemistry of Non-Stoichiometric Pentavalent Vanadium Oxides: Crystal Structure of $Li_{1+x}V_3O_8$*, Acta Cryst., **10**, 261-267 (1957).
30. L. A. de Picciotto, K. T. Adendorff, D. C. Liles and M. M. Thackeray, *Structural Characterisation of $Li_{1+x}V_3O_8$ Insertion Electrodes by Single-Crystal X-ray Diffraction.* Solid State Ionics, **62**, 297-307 (1993).
31. R. Benedek, M. M. Thackeray and L. H. Yang, *Lithium Site Preference and Electronic Structure of $Li_4V_3O_8$*, Phys. Rev. B, **56**, 10707-10710 (1997).
32. R. Benedek, M. M. Thackeray and L. H. Yang, *Atomic Structure and Electrochemical Potential of $Li_{1+x}V_3O_8$*, Phys. Rev. B, **60**, No.6, 1-8 (1999).
33. L. A. de Picciotto and M. M. Thackeray, unpublished data.
34. M. M. Thackeray, W. I. F. David, P. G. Bruce and J. B. Goodenough, *Lithium Insertion into Manganese Spinels*, Mat. Res. Bull., **18,** 461-472 (1983).

35. M. M. Thackeray, P. J. Johnson, L. A. de Picciotto, P. G. Bruce and J. B. Goodenough, *Electrochemical Extraction of Lithium from $LiMn_2O_4$,* Mat. Res. Bull., **19,** 179-187 (1984).
36. T. Ohzuku, M. Kitagawa and T. Hirai, *Electrochemistry of Manganese Dioxide in Lithium Nonaqueous Cell*, J. Electrochem. Soc., **137**, 769-775 (1990).
37. J. M. Tarascon and D. Guyomard, *Li Metal-Free Rechargeable Batteries Based on $Li_{1+x}Mn_2O_4$ Cathodes ($0 \leq x \leq 1$) and Carbon Anodes*, J. Electrochem. Soc., **138**, 2864-2868 (1991).
38. M. M. Thackeray, *Manganese Oxides for Lithium Batteries*, Progress in Solid State Chem., **25**, 1-71 (1997).
39. J. B. Goodenough, M. M. Thackeray, W. I. F. David and P. G. Bruce, *Lithium Insertion/Extraction Reactions with Manganese Oxides*, Rev. de Chim. Min., **21,** 435-455 (1984).
40. R. J. Gummow, A. de Kock and M. M. Thackeray, *Improved Capacity Retention of Lithium Manganese Oxide Spinel Cathodes in Lithium Cells*, Solid State Ionics, **69**, 59-67 (1994).
41. M. M. Thackeray, A. de Kock, M. H. Rossouw, D. C. Liles, D. Hoge and R. Bittihn, *Spinel Electrodes from the Li-Mn-O System for Rechargeable Lithium Battery Applications,* J. Electrochem. Soc., **139**, 363-366 (1992).
42. D. Guyomard and J. M. Tarascon, *The Carbon/$Li_{1+x}Mn_2O_4$ System*, Solid State Ionics, **69**, 222-237 (1994).
43. D. Aurbach and Y. Gofer, *The Behavior of Lithium Electrodes in Mixtures of Alkyl Carbonates and Ethers*, J. Electrochem. Soc., **138**, 3529-3535 (1991).
44. D. Aurbach, A. Zaban, A. Schlecter, Y. Ein-Eli, E. Zenigard and B. Markowsky, *The Study of Electrolyte Solutions Based on Ethylene and Diethyl Carbonates for Rechargeable Li Batteries*, J. Electrochem. Soc., **142**, 2873-28882 (1995).
45. J. C. Hunter, *Preparation of a New Crystal Form of Manganese Dioxide: λ-MnO_2*, J. Solid State Chem., **39**, 142-147 (1981).
46. M. M. Thackeray, Y. Shao-Horn, A. J. Kahaian, K. D. Kepler, E. Skinner, J. T. Vaughey and S. A. Hackney, *Structural Fatigue in Spinel Electrodes in High-Voltage (4 V) Li/$Li_xMn_2O_4$ Cells,* Electrochem. and Solid State Letters, **1**, 7-9 (1998).
47. J. Cho, G. Kim and M. M. Thackeray, *Structural Changes of $LiMn_2O_4$ Spinel Electrodes During Electrochemical Cycling*, J. Electrochem. Soc., (1999). In press.

Captions to Figures

Figure 1. The ideal structures of a) graphite and b) lithiated graphite LiC_6. The dashed lines in (a) represent C_6 hexagons above and below the plane of C_6 hexagons defined by solid lines.

Figure 2. a) Cubic InSb (zinc-blende-type structure), b) a [110] projection of InSb, and c) the predicted structure of Li_2InSb [12].

Figure 3. a) The $A[B_2]O_4$ spinel structure, A= tetrahedral-site cations, B= octahedral-site cations, and b) the lithiated spinel structure $LiA[B_2]O_4$ with a rock salt configuration.

Figure 4. The ideal $LiNiO_2$ structure.

Figure 5. The structures of a) $Li_{1.2}V_3O_8$ and b) $Li_4V_3O_8$ (• = Li, o = O). The vanadium ions (not marked) are located within the oxygen polyhedra.

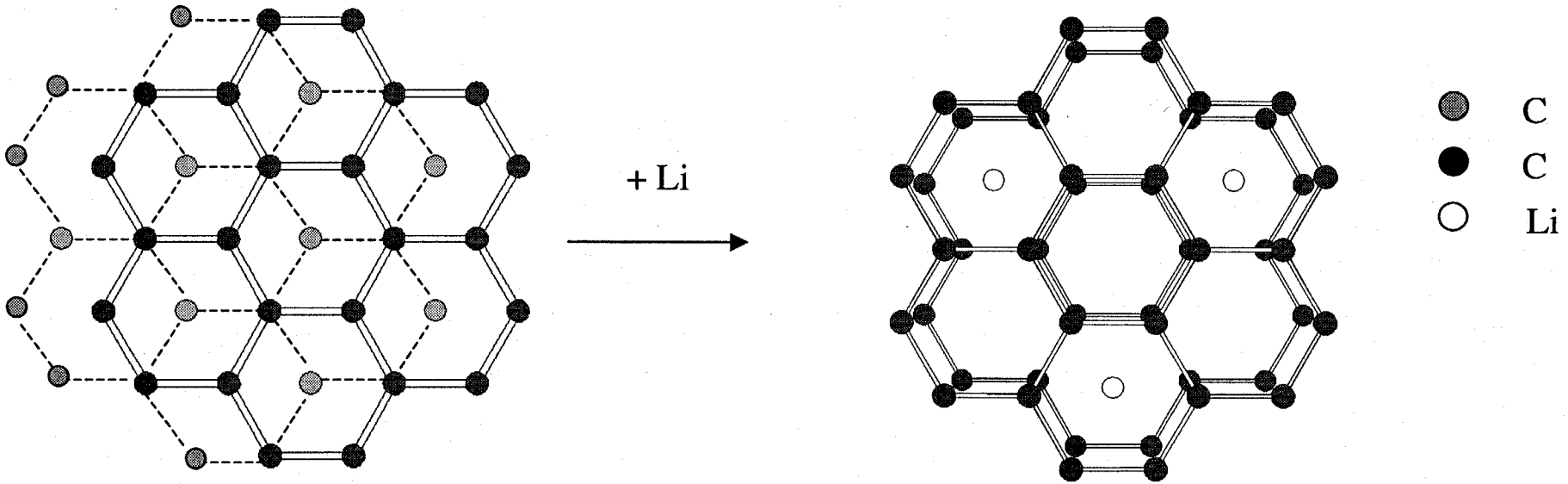

Figure 1

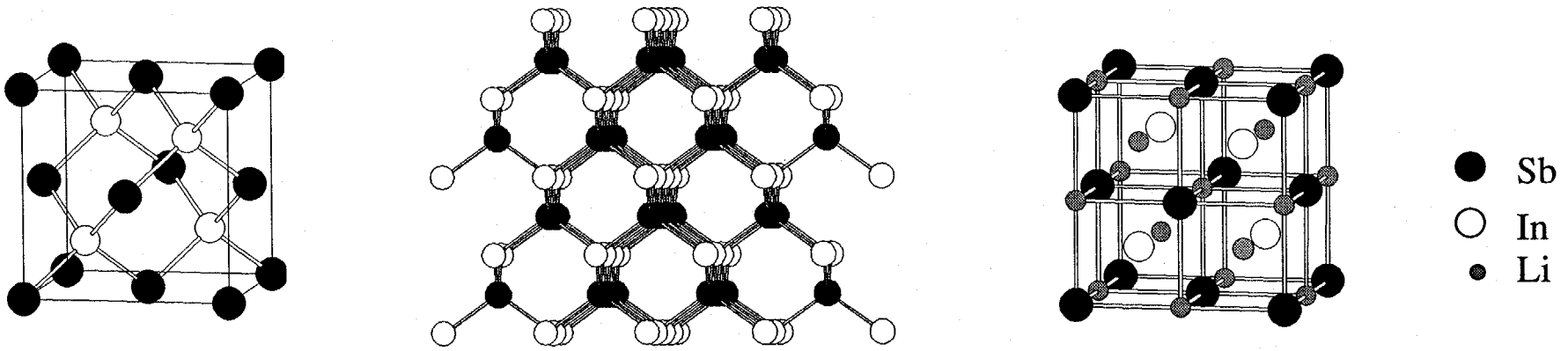

(a) (b) (c)

Figure 2

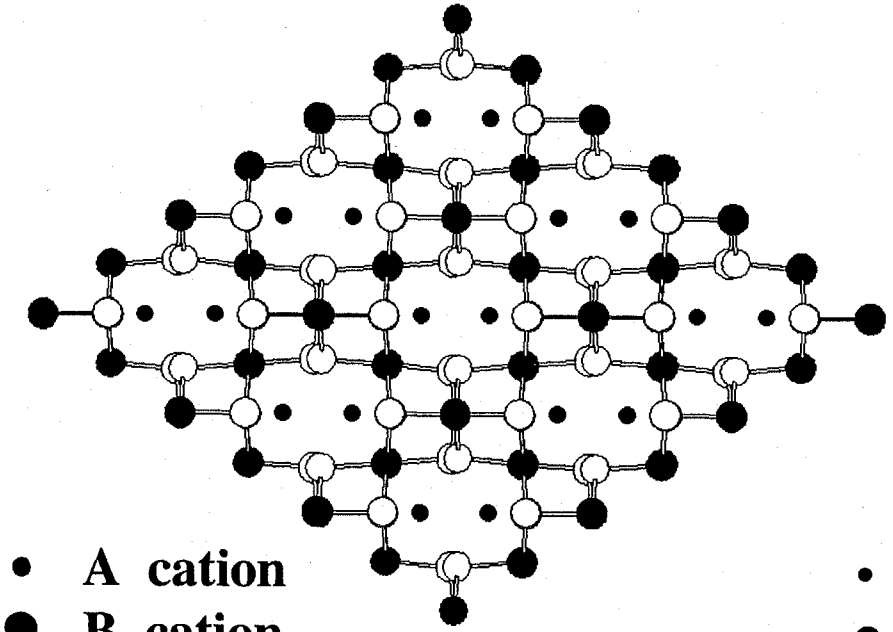

• A cation
● B cation
○ O anion

(a)

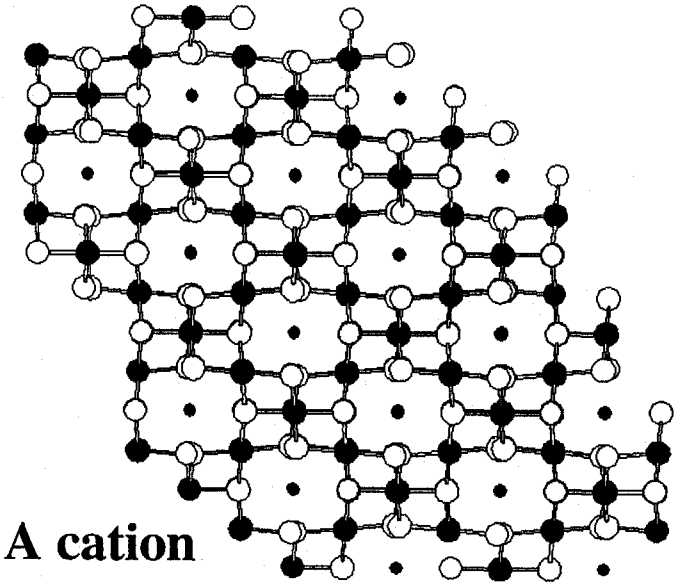

• Li and A cation
● B cation
○ O anion

(b)

Figure 3

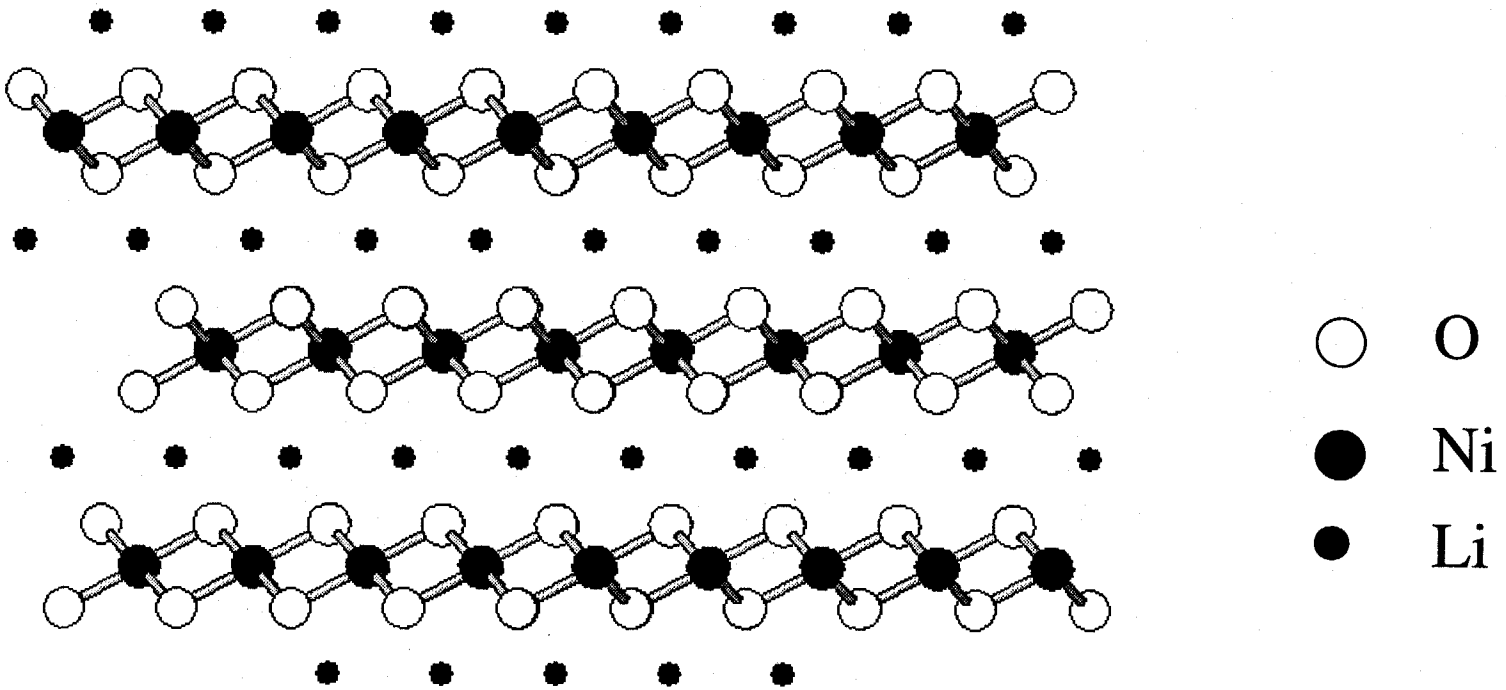

Figure 4

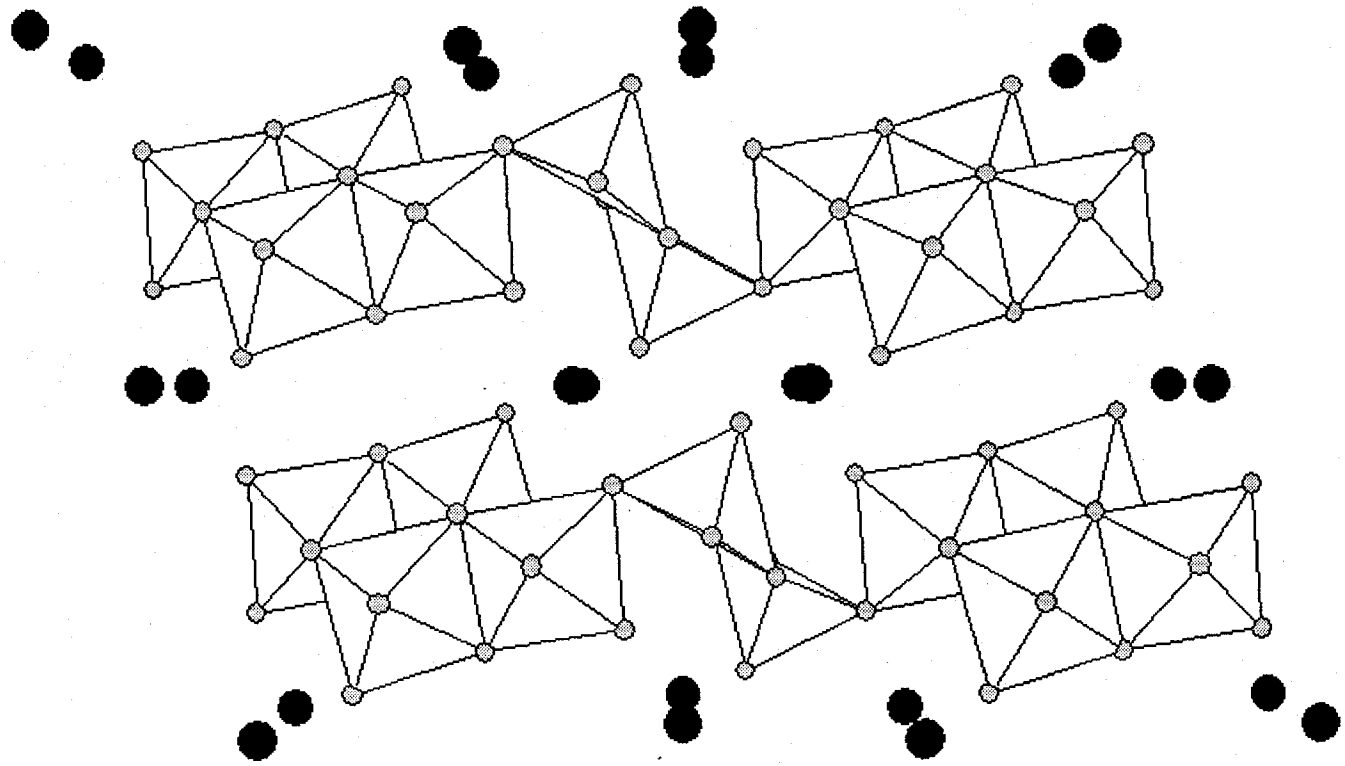

Figure 5a

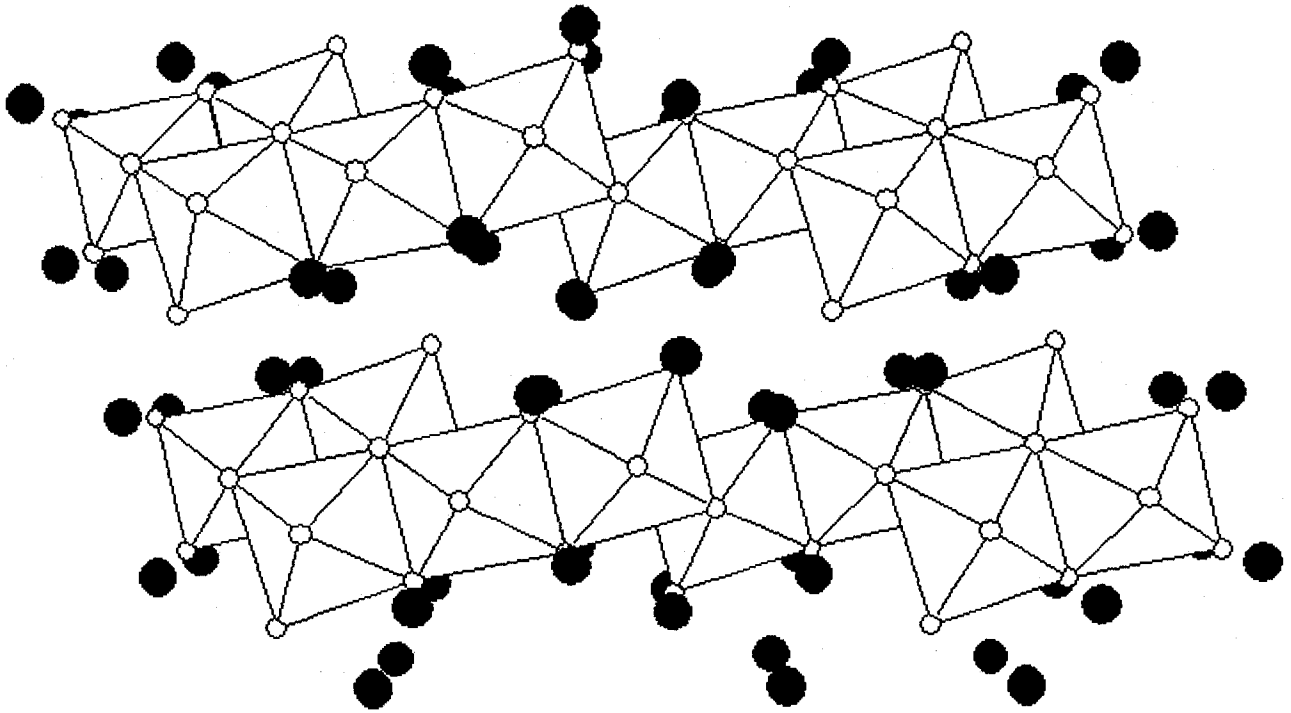

Figure 5b